THE JOURNAL OF PHYSICAL CHEMISTRY B

ARTICLE

pubs.acs.org/JPCB

Characterization of Composite Phthalocyanine−Fatty Acid Films from the Air/Water Interface to Solid Supports

G. Giancane,*[,†] D. Manno,[‡] A. Serra,[‡] V. Sgobba,[§] and L. Valli[†]

[†]Dipartimento di Ingegneria dell'Innovazione, Università degli Studi del Salento, I-73100 Lecce, Italy

[‡]Dipartimento di Scienze dei Materiali, Università degli Studi del Salento, I-73100 Lecce, Italy

[§]Department of Chemistry and Pharmacy & Interdisciplinary Center for Molecular Materials, Friedrich-Alexander-Universität Erlangen-Nürnberg, Egerlandstrasse, 3, D-91058 Erlangen, Germany

ABSTRACT: A commercial vanadyl 2,9,16,23-tetraphenoxy-29H,31H-phthalocyanine (VOPc) was dissolved in chloroform and spread on ultrapure water subphase in a Langmuir trough. The floating film was thoroughly characterized at the air−water interface by means of the Langmuir isotherm, Brewster angle microscopy, UV−vis reflection spectroscopy, and infrared measurements carried out directly at the air−water interface. All the results showed the formation of a non-uniform and aggregated floating layer, too rigid to be transferred by the Langmuir−Blodgett (LB) method. For this reason, a mixture of arachidic acid and VOPc was realized, characterized, and transferred by the LB technique on solid substrates. Interface measurements and atomic force microscopy analysis suggested the formation of a uniform arachidic acid film and a superimposed VOPc placed in prone configuration.

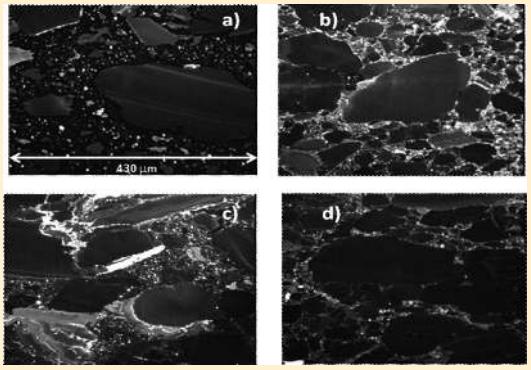

INTRODUCTION

Chemical and physical properties of phthalocyanines (Pc's) have always attracted the attention of numerous researchers for the diversified applications of these molecules in miniaturized electronic devices such as chemical sensors,[1,2] organic field effect transistors,[3] solar cells,[4] electrochromic[5] and thermochromic apparatuses,[6] laser dyes[7] and many other applications even in the biomedical field,[8] such as in photodynamic cancer therapy.[9] Most of these applications usually stem from the Pc wide flat π-electron cloud, which is responsible of the typical blue-green color of these materials. Pc's comply with the fundamental requisites of chemical and light resistance and mechanical and thermal stability (they are usually sublimed at a temperature of about 500 °C in vacuum, condensing unaltered), all essential for active layers in functioning devices. In the majority of these applications, outstanding performances are observed in highly oriented films obtained by selected film construction techniques. In comparison with methods currently employed in the majority of inorganic systems, the present construction of organic apparatuses can be easier, environmentally more friendly, and, above all, economical when commercially available materials (such as the one employed in this research) are used. Among them, several deposition methods can be used to obtain films of Pc's; some of the most appealing are self-organization techniques, such as the Langmuir−Blodgett (LB) or Langmuir−Schäfer (LS), self-assembly or layer-by-layer approaches.[10,11] They represent an alternative cost-effective, solution-based transferring method that gives the possibility to tune at the nanometric level the molecular composition, architecture, and thickness of the Pc film. The use of such immobilization methods is necessary since it is well-known that some frontier applications require organized layers of molecular dimensions. Above all, the LB technique is an economic but time-consuming method that allows one to transfer a wide typology of organic materials; the horizontal lifting variation (LS method) offers the chance to construct more rapidly multilayers of organic materials. Organized monolayers of Pc's can be obtained by the attachment of adequate substituents to control the floating film−subphase interaction and to tailor peculiar properties such as light absorption, conductivity, distribution of energy levels, etc. Nevertheless, sometimes the floating layers of Pc's appear inhomogeneous and patchy and with small values of the limiting areas per molecule that are not consistent with the formation of a real monolayer. Therefore, floating films have been also prepared using a mixture of the investigated Pc with arachidic acid (AA), a well-known film-forming material largely used to promote organized LB and LS films.

Concerning vanadyl Pc's, an extensive collection of patent literature exists regarding their employment as potential optical recording agents,[12] photoreceptors,[13] transistors,[14] and nonlinear optics devices.[15] In this work, a commercial tetra-substituted vanadyl Pc, vanadyl-2,9,16,23-tetraphenoxy-29*H*, 31*H*-phthalocyanine (here hence named VOPc) has been characterized and transferred onto solid substrates as is and in mixture

Received: September 21, 2011
Revised: November 7, 2011
Published: November 09, 2011

with AA. The corresponding floating films have been investigated at the air−water interface by non-conventional techniques, such as UV−vis reflection spectroscopy, polarization−modulation infrared reflection−absorption spectroscopy, and Brewster angle microscopy (BAM), in addition to Langmuir curves. The transferred films have been characterized by Raman spectroscopy, atomic force microscopy (AFM) and X-ray diffraction (XRD). In the case of AA/VOPc mixed films, all data are consistent with the generation of a fatty acid layer with Pc molecules superimposed prone on the hydrophobic bed created by the hydrocarbon tails of AA. AFM and XRD measurements are consistent with the formation of highly oriented multilayers; within the mixed films, two different regions with distorted orthorhombic subcell packing are evidenced.

EXPERIMENTAL METHODS

All chemicals were purchased from Sigma-Aldrich and used without further purification.

LB depositions were carried out by a KSV 5000 Langmuir trough. Reflection spectroscopy and BAM analysis were carried out using a NIMA 601BAM apparatus. BAM was mounted directly above a Langmuir trough. It was fitted with a 10× long working distance objective lens, and both the objective and the detector were mounted at the Brewster angle for water at 532 nm of 53.15°. The field of view of the lens was approximately 440 μm × 330 μm with a resolution of approximately 2 μm. A piece of angled black glass was mounted at the bottom of the trough to ensure that no double reflection from the laser could occur. The reflection data (ΔR) were obtained on an NFT ref Spec instrument. They were acquired under normal incidence of radiation according to the description given in reference 16 and corresponding to the difference between the reflectivities of the floating film−liquid interface and the clean air−liquid interface. BAM measurements were obtained on an NFT BAM2plus system. A polarization modulation infrared reflection absorption spectroscopy (PM-IRRAS) 550 Fourier-transformation infrared reflection absorption measurement system, KSV, was employed to investigate the spread compound properties in the infrared spectral range.

UV−visible investigation on the Pc derivative in chloroform solution was realized by a Lambda 650 Perkin-Elmer spectrometer, and the LB films were deposited onto previously hydrophobized quartz plates. The AFM experiments were performed by means of a Jeol 4200 scanning probe. Finally, XRD measurements were realized by a RIGAKU D/MAX-Ultima+. Raman measurements were carried out by means of a Renishaw Invia with a 514.5 nm excitation laser.

The chemical structure of the commercial VOPc is reported in Scheme 1.

RESULTS AND DISCUSSION

Characterization of VOPc Floating Films at the Air−Water Interface. Tetrasubstituted VOPc was dissolved in chloroform with a concentration of 3×10^{-4} M, and an aliquot of 200 μL was spread onto an ultrapure water Milli-Q grade subphase by means of a microsyringe.

After the solvent evaporation, the floating film was compressed by moving the Teflon barriers of the Langmuir trough, and the surface pressure Π of the floating film was monitored by means of a Wilhelmy plate. In Figure 1, the isotherm curve of the

Scheme 1. Chemical Structure of VOPc

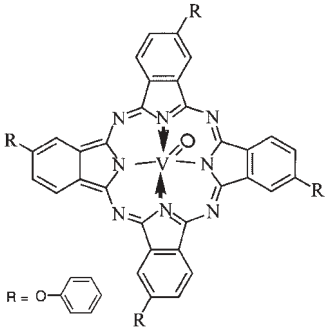

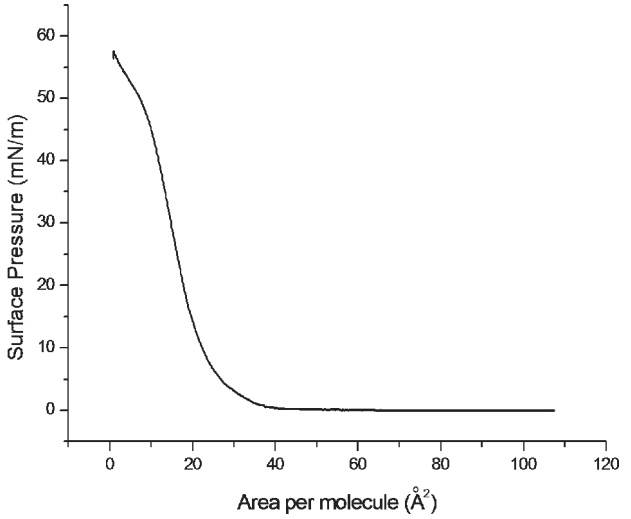

Figure 1. Isotherm curve surface pressure versus area per molecule of VOPc.

spread molecules is reported, and a wide portion of the curve can be ascribed to the pseudogaseous phase of the floating film at low surface pressure values followed by a rapid slope variation that introduces the VOPc in the "condensed"-like phase. This behavior is characteristic of not-fully amphiphilic molecules.[17] Cyclic compressions of the barriers of Langmuir trough point out the strong hysteresis of the VOPc floating film, suggesting that a rigid layer covers the subphase.

The extrapolation of the linear portion of the Langmuir curve to 0 mN/m gave a value of the limiting area per molecule of VOPc of ∼22 Å^2/molecule, and it is considerably smaller than the theoretical value of about 60 Å^2/molecule for an edge-on organization of macrocycles within the monolayer at the air−water surface. Thus it can be supposed that the spread molecules form aggregates at the air−water interface. In order to corroborate such a hypothesis, reflection spectra were acquired directly for the floating film. The Q_1 band of the monomeric form, detectable at 700 nm for the absorption spectrum of VOPc in chloroform solution (see inset of Figure 2), is 70 nm red-shifted in comparison with the Q_2 band of the aggregated form at 630 nm; on the contrary, the Q_1 band at the air/water interface is totally absent, and the Q_2 band is evident at 605 nm. The consequent rationale is that the floating film is mainly constituted by aggregated domains.[18]

A further confirmation of the strong aggregation of the spread molecules is suggested also by BAM performed on the floating

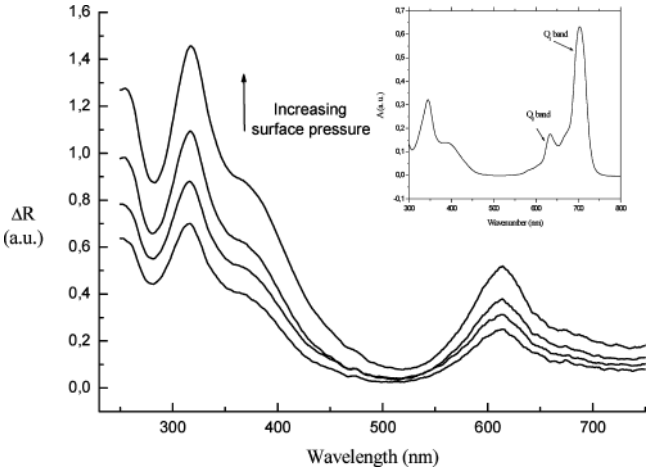

Figure 2. Reflection spectra of a VOPc floating film at different surface pressures; in the inset, the absorption spectrum of a chloroform solution of VOPc is reported.

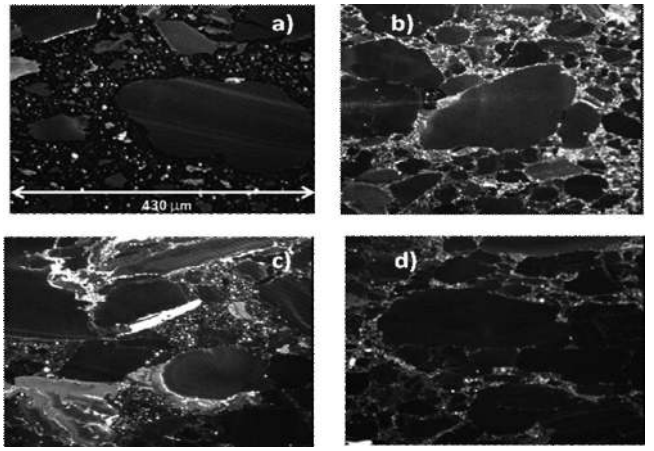

Figure 3. BAM pictures taken for increasing surface pressure values: (a) 1 mN/m, (b) 5 mN/m, (c) 11 mN/m, (d) 22 mN/m.

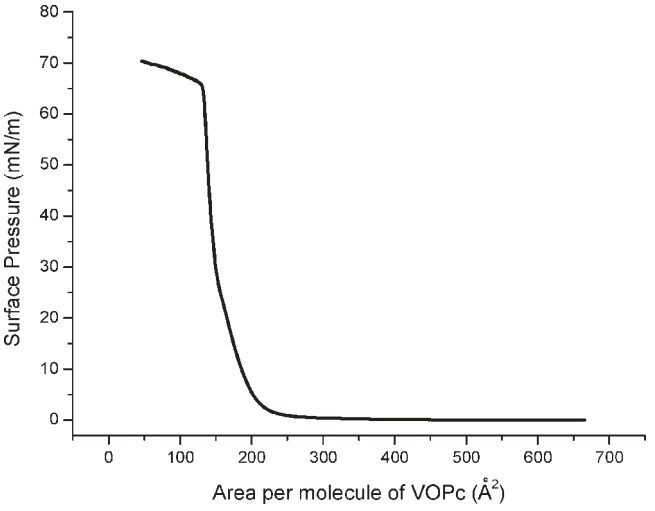

Figure 4. Langmuir curve of VOPc/AA in a molar ratio of 1:4, respectively.

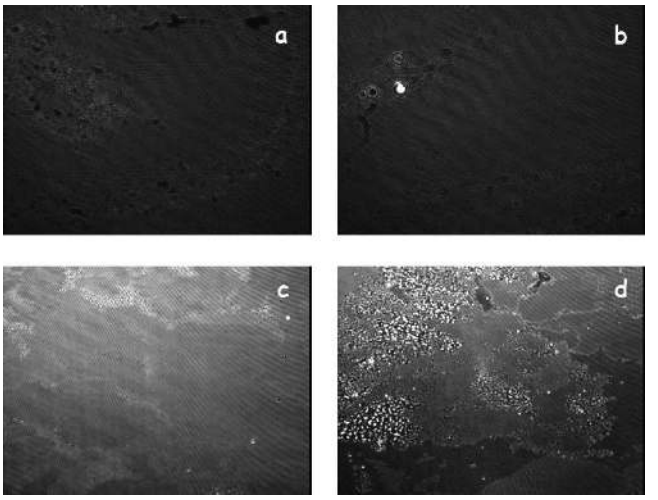

Figure 5. BAM pictures of the AA/VOPc composite floating film recorded for increasing surface pressures: 1 mN/m (a), 8.5 mN/m (b), 22 mN/m (c), and 40 mN/m (d).

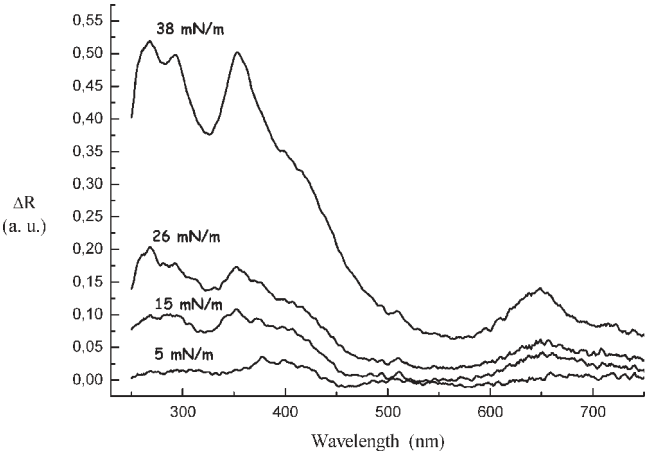

Figure 6. Reflection spectra at the air−water interface of the compound VOPc mixed with AA in a molar ratio of 1:4, respectively.

film during the barriers motion of the Langmuir trough. In Figure 3a, the BAM picture of the floating film at 1 mN/m shows the simultaneous presence of large aggregates and noncovered subphase regions. Furthermore, some aggregates are shaped with edges, corners, and with different shades of gray, indicating that the floating layer is formed by domains with different thickness and orientation. By increasing the surface pressure, coalescence of the floating domains and the generation of larger, rigid, and tridimensional aggregated ones can be observed (Figure 3b,c,d).

In order to obtain more uniform floating films and to prevent the formation of molecular aggregates, molecular spacers such as AA or octadecylamine can be used in different molar ratios.[19,20]

Characterization of Composite VOPc−AA Floating Film at the Air−Water Interface. A mixture of VOPc and AA in a molar ratio of 1:4 was spread on a subphase containing $CdCl_2$ 0.5 mM and KOH 0.2 mM dissolved in ultrapure water.[21] The isotherm curve of the VOPc/AA mixture (Figure 4) shows a limiting area of about 200 $Å^2$ in the range of surface pressure between 7 and 25 mN/m, and it decreases to 160 $Å^2$ for higher surface pressure values comparable to a planar arrangement of the Pc aggregates.

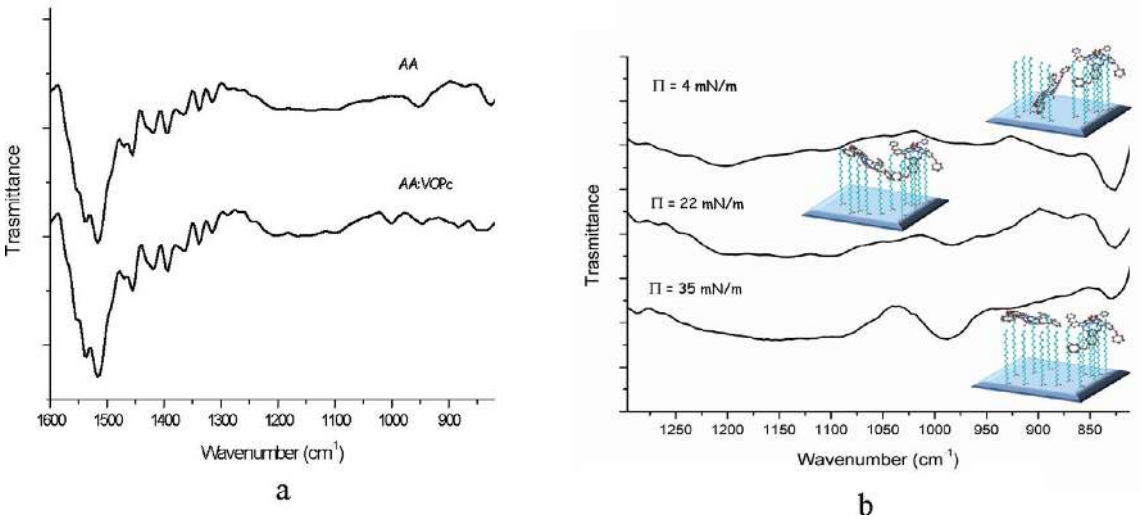

Figure 7. (a) PM-IRRAS spectra of AA and AA/VOPc floating films; (b) PM-IRRAS spectra of AA/VOPc floating films at different surface pressures. In the inset of panel b, the molecular arrangement at the air/water interface is proposed.

This slope variation observed at 30 mN/m can be rationalized as a reorganization of the AA and VOPc domains at the air/water interface. The molecules of AA are probably densely packed on the water surface, while, upon compression, the Pc molecules have been gradually squeezed out of the fatty acid layer. Subsequent investigations (vide infra) are consistent with this rationale.

BAM images of the cospread VOPc/AA mixture acquired during the barrier motion (Figure 5) are remarkably different from the pictures reported for the pure VOPc. The floating layer appears uniform and homogeneous already at low pressures, and the morphology suddenly changes in correspondence to the slope variation in the isotherm curve. Again such a behavior can be explained supposing that at high Π the VOPc aggregates are pushed out of the AA matrix, and a further increment of the barrier pressure induces the formation of an overlapped multilayer, with AA molecules in direct contact with the polar aqueous subphase and the VOPc macrocycles distributed prone on the hydrophobic terminations of the hydrocarbon tails of the fatty acid.

A further confirmation of this rationale is suggested by the reflection spectra at the air−water interface in Figure 6. Comparing ΔR values of the floating film compressed at 38 mN/m with the spectrum related to the layer at 26 mN/m, a strong enhancement of spectrum intensity can be observed; on the contrary, the signals recorded at lower surface pressures are comparable. Moreover, it is interesting to observe that the Q-band, located at 650 nm, is 35 nm shifted if compared with reflection spectra of pure VOPc. This signal can be attributed to the Q_1 band, which represents the Pc monomeric form, confirming the well-known film promoting properties of fatty acid molecules. Such a shift is preserved when the floating film is transferred onto the solid substrate, suggesting that the observed behavior at the air/water interface is preserved also on the solid film.

PM-IRRAS was carried out directly on the floating film, and the vibrational spectra were acquired at different values of surface pressure. This technique allows one to identify the spatial arrangement of functional groups at the interface: if the orientation of a transition moment is parallel to the surface plane, the PM-IRRAS signal is equal to zero; on the contrary, if the orientation is perpendicular to the surface plane, the signal is maximum.[22,23] Signals recorded in the PM-IRRAS spectra can be mainly assigned to AA vibrational modes (the AA concentration is 4 times higher than the one of VOPc), but the band at 997 cm^{-1} (Figure 7a) is ascribed to the V═O vibrational modes of the Pc derivative.[24−26] Infrared spectra acquired at different surface pressures (Figure 7b) show an increase of this signal, suggesting that high surface pressure values induce a horizontal arrangement of VOPc macrocycles over the AA film, forming an overimposed layer of VOPc on the AA matrix.

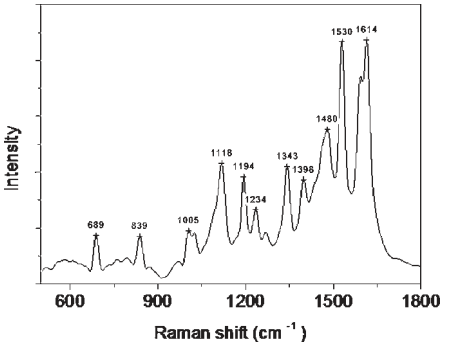

Figure 8. Raman shift of a 20-layer LB film of VOPc/AA blend transferred on a glass substrate.

We wish to stress that the rationale drawn in this work has also been previously suggested by other researchers; in fact, a rather flat orientation of the tetrapyrrolic macrocycles in mixed monolayer assemblies with respect to the subphase surface was also claimed by Lesieur and Möbius.[27]

Raman Spectroscopy of LB Composite Films. Raman scattering provides thorough structural and electronic information about Pc's in situ in biological environments, onto metal surfaces, in pigments, in the solid state, and in solution.[28]

The Raman spectrum of a 25-layer film of AA/VOPc on glass is reported in Figure 8. The Raman bands have been assigned using model compounds such as benzene, pyrrole, and Pc's. As reported in the literature,[29] vanadyl Pc belongs to the point group

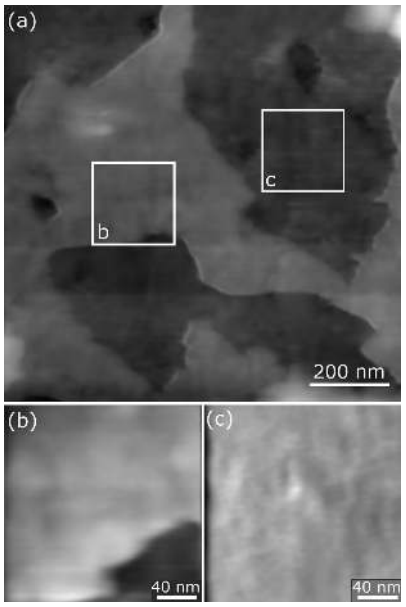

Figure 9. AFM image at low magnification (a) and higher magnification (b,c).

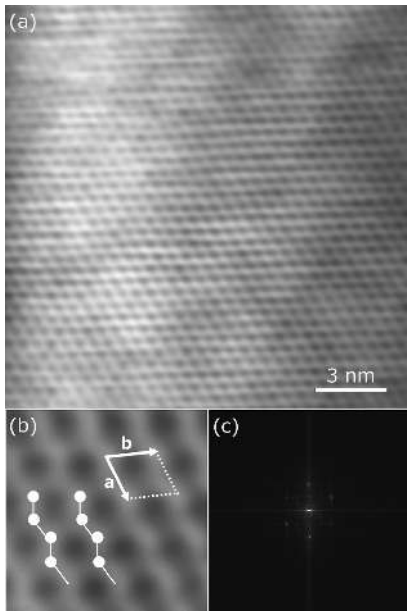

Figure 10. High-resolution AFM image (a) obtained from the region imaged in Figure 9b, enlargement (b), and FFT picture (c).

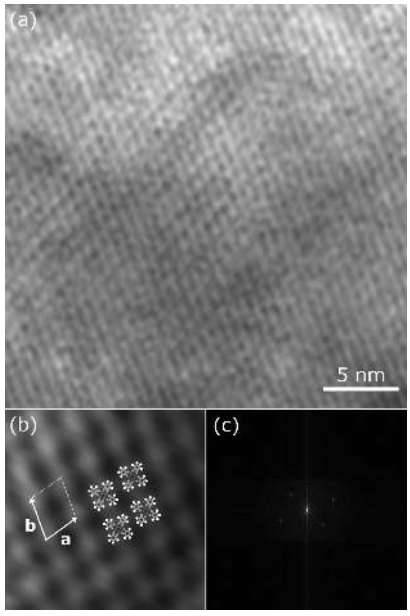

Figure 11. High-resolution AFM image (a) obtained from the region imaged in Figure 9c, enlargement (b), and FFT picture (c).

C_{4v}, and, since there are 58 atoms, 168 $(3n - 6)$ vibrations are expected. The irreducible representation consists of the following species: $23a_1 + 19a_2 + 21b_1 + 21b_2, + 42e$ (doubly degenerate). On the basis of C_{4v} symmetry, the a and e species are both Raman- and IR-active, while the b_1 and b_2 species are Raman-active only. The a_2 species are neither Raman- nor IR-active.

According to Raman depolarization ratios theory,[30] vanadyl Pc films have very strong bands at 1530 and 1614 cm^{-1}, while the intensities of other bands are significantly lower. The bands at 1530 and 1343 cm^{-1} are due to pyrrole stretching modes. Vibrations associated with carbon−carbon stretching in benzene rings are observed at 1614 cm^{-1}. Carbon−hydrogen bending bands, normally weak in the Raman spectrum of Pc molecules, were observed in the 1200−1100 cm^{-1} spectral range. The macrocycle refers to the inner core of Pc, which consists of 16 alternating carbon and nitrogen atoms which are conjugated. The Raman bands at the 839−689 cm^{-1} spectral range are assigned in Pc molecules to the macrocycle breathing vibration and a collective stretching vibration of the macrocycle.

AFM Characterizations of LB Composite Films. A film consisting of two layers of VOPc/AA blend (1:4 molar ratio, respectively) was transferred on a glass substrate by the LB technique at 26 mN/m, and it was observed by means of AFM. The thin film consists of two different regions, as shown in Figure 9, recorded at low magnification.

The two regions, magnified in Figures 9b,c are characterized by a different roughness, with values of 0.12 and 0.45 nm, respectively.

Molecular resolution AFM images were obtained for the two regions of Figure 9. Figure 10 shows a typical high-resolution AFM image obtained from the region imaged in Figure 9b. The lighter part of the image indicates the upper region of the surface, and the darker areas correspond to deeper ones. A two-dimensional periodic structure at molecular resolution is clearly discernible. Rows of chain ends appear at approximately 45° to the horizontal AFM scan direction, as evidenced in the enlargement shown in Figure 10b. This is consistent with the dipping direction during the LB transfer of the floating film, as already observed also in the case of differently functionalized copper Pc's.[31−33] In order to measure the periodicity observed in the AFM image, two-dimensional fast Fourier transform (FFT) analysis was undertaken. Figure 10c shows the corresponding FFT spectrum. Inspection of the image reveals six bright spots. This is similar to that reported previously for LB films of cadmium arachidate.[34,35] However, thorough examination of the pattern of spots suggests an oblique, rather than a rectangular, unit cell. Our rationale is a molecular organization based on a distorted orthorhombic subcell packing; the unit cell parameters,

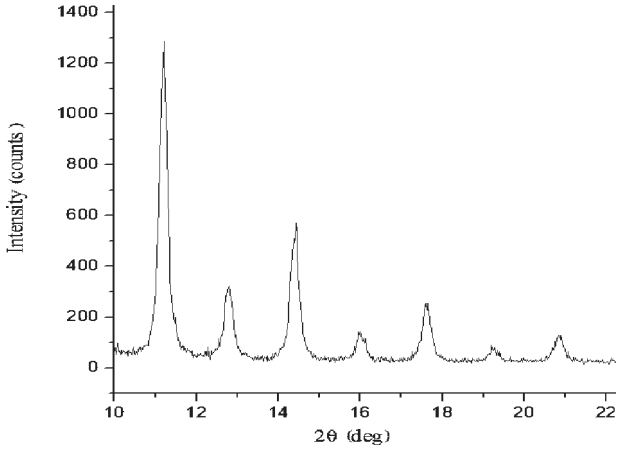

Figure 12. XRD pattern of 30 layers of the LB film of AA/VOPc.

Table 1. XRD Data: Experimental 2θ and Corresponding Interplanar Spacing *d* Compared with the Values of 2θ and *d* Coming from a Simulation Based on the Bidimensional Cells Hypothesized According to AFM Results for the Vanadyl Pc Derivative and AA Films

XRD data		vanadyl Pc a = 0.825 nm, b = 0.720 nm γ = 73 deg			AA a = 0.568 nm, b = 0.520 nm γ = 77 deg		
2θ (deg)	d (nm)	2θ (deg)	d (nm)	h,k	2θ (deg)	d (nm)	h,k
11.21	0.789	11.2	0.79	1,0			
12.75	0.694	12.7	0.69	0,1			
14.37	0.616	14.3	0.62	1,1			
15.99	0.554				16.0	0.55	1,0
17.63	0.502				17.5	0.51	0,1
19.25	0.460	19.3	0.46	−1,1			
20.82	0.426				20.9	0.42	−1,1

a and **b**, are labeled in Figure 10b: **a** = 0.568 nm, **b** = 0.520 nm and form an angle of 77°.

Comparable AFM images were obtained from the other region of Figure 9. Figure 11a shows a typical AFM image obtained from the region imaged in Figure 9c. Also in this case, the lighter areas of the image indicates the upper part of the surface, and the darker regions correspond to deeper ones. A different two-dimensional periodic structure at molecular resolution is clearly discernible (Figure 11b). In order to measure the periodicity contained within the AFM image, another two-dimensional FFT analysis was again undertaken. Figure 11c shows the FFT spectrum corresponding to the image shown in Figure 11a. Inspection of the image reveals four bright spots and two additional faint ones. An explanation of such molecular organization can be based onto a distorted orthorhombic subcell packing, with one molecule unit cell. The unit cell parameters, **a** and **b**, are labeled in Figure 11b. In addition, it was calculated that **a** is 0.825 nm and **b** is 0.720 nm. The angle between the vectors **a** and **b** was estimated to be 73°.

The interpretation of molecular arrangement was completely confirmed by XRD carried out on two LB layers of VOPc. The XRD spectrum obtained from the analyzed film is reported in Figure 12.

Table 1 reports the experimental XRD data, and the values of 2θ and *d* coming from a simulation based on the cells hypothesized according to AFM results.

As is clearly evident, the XRD data are in excellent agreement with the theoretical values and confirm the results obtained from AFM high-resolution observations.

CONCLUSIONS

A tetrasubstituted V═O Pc (VOPc) has been investigated in Langmuir experiments. The floating film appeared to be, from the BAM investigations, very rigid, and bands attributable to three-dimensional aggregates were revealed by means of reflection spectroscopy at the air−water interface. Therefore, VOPc was mixed with a film promoter, in this case AA, in a molar ratio of 1:4, respectively. The resulting floating film appeared to be uniform, and monomeric Q_1 bands were exhibited in the reflection spectra. Moreover, PM-IRRAS measurements on these composite floating films suggest that a homogeneous AA layer was generated during the barrier motion, and the VOPc domains were forced out on the AA film, increasing the surface pressure. Films of the AA/VOPc blend were transferred onto solid substrates by the LB technique, and high-resolution AFM images showed that the presence of the AA layer promoted the formation of a highly oriented overimposed VOPc layer.

REFERENCES

(1) Mabeck, J. T.; Malliaras, G. G. *Anal. Bioanal. Chem.* **2006**, *384* (2), 343–353.

(2) Zhou, R.; Josse, F.; Gopel, W.; Ozturk, Z. Z.; Bekaroglu, O. *Appl. Organomet. Chem.* **1996**, *10* (8), 557–577.

(3) Cicoira, F.; Coppede, N.; Iannotta, S.; Martel, R. *Appl. Phys. Lett.* **2011**, *98*, 183303/1–183303/3.

(4) Peumans, P.; Uchida, S.; Forrest, S. R. *Nature* **2003**, *425*, 158–162.

(5) Nagel, S.; Lener, M.; Keil, C.; Gerdes, R.; Lapok, L.; Gorun, S. M.; Schlettwein, D. *J. Phys. Chem. C* **2011**, *115*, 8759–8767.

(6) Pan, Y. L.; Wu, Y. J.; Chen, L. B.; Zhao, Y. Y.; Shen, Y. H.; Li, F. M.; Shen, S. Y.; Huang, D. H. *Appl. Phys. A: Mater. Sci. Process.* **1998**, *66*, 569–573.

(7) Reda, S. M. *Sol. Energy* **2007**, *81*, 755–760.

(8) Nishiyama, N.; Iriyama, A.; Jang, W. D.; Miyata, K.; Itaka, K.; Inoue, Y.; Takahashi, H.; Yanagi, Y.; Tamaki, Y.; Koyama, H.; Kataoka, K. *Nat. Mater.* **2005**, *4*, 934–941.

(9) Li, L.; Chen, J.-Y.; Wu, X.; Wang, P.-N.; Peng, Q. *J. Phys. Chem. B* **2010**, *114*, 17194–17200.

(10) Petty, M. C. *Langmuir−Blodgett Films: An Introduction*; Cambridge University Press: Cambridge, U.K., 1996. Petty, M. C. *Molecular Electronics from Principles to Practise*; Wiley: Chichester, U.K., 2007. Roberts, G. *Langmuir−Blodgett Films*; Plenum Press: New York, 1990. Tredgold, R.H. *Order in Thin Organic Films*; Cambridge University Press: Cambridge, U.K., 1994. Ulman, A. *An Introduction to Ultrathin Organic Films from Langmuir−Blodgett to Self-Assembly*; Academic Press: San Diego, CA, 1991. Valli, L. *Adv. Colloid Interface Sci.* **2005**, *116* (2005), 13–44.

(11) Kumaran, N.; Veneman, P. A.; Minch, B. A.; Mudalige, A.; Pemberton, J. E.; O'Brien, D. E.; Armstrong, N. R. *Chem. Mater.* **2010**, *22*, 2491–2501.

(12) Aoki, M.; Kaieda, O.; Masuda, K.; Okumura, Y., PCT Int. Appl. (1998), WO 9816588 A119980423. Yu, H.; Ye, Q.; Li, X.; Huang, D.; Liu, Y. *Proceedings of SPIE-The International Society for Optical Engineering*; 2890 (Optical Recording, Storage, and Retrieval Systems); 1996; pp 108−114.

(13) Wang, Y.; Liang, D. *Adv. Mater. (Weinheim, Germany)* **2010**, *22*, 1521–1525.

(14) Pan, F.; Tian, H.; Qian, X.; Huang, L.; Geng, Y.; Yan, D. *Org. Electron.* **2011**, *12*, 1358–1363.
(15) Jin, Y. L.; Jiang, Q.; Ito, Y.; Maeda, A.; Furuhashi, H.; Yoshikawa, T.; Uchida, Y.; Kojima, K.; Ohashi, A.; Ochiai, S.; et al. *Proceedings of SPIE-The International Society for Optical Engineering*; 4580 (Optoelectronics, Materials, and Devices for Communications); 2001; pp 380−390.
(16) Grüniger, H; Möbius, D; Meyer, H. *J. Chem. Phys.* **1983**, *79*, 3701–3710.
(17) Tredgold, R. H. *Rep. Prog. Phys.* **1987**, *50*, 1609–1656. Ingrosso, C.; Curri, M. L.; Fini, P.; Giancane, G.; Agostiano, A.; Valli, L. *Langmuir* **2009**, *25*, 10305–10313.
(18) Barszcz, B; Bogucki, A.; Biadasz, A.; Bursa, B.; Wróbel, D.; Graja, A. *J. Photochem. Photobiol. A* **2011**, *218*, 48–57.
(19) Sheu, C.-W.; Lin, K.-M.; Ku, I.-H.; Chang, C.-H.; Lee, Y.-L.; Yang, Y.-M.; Maa, J.-R. *Colloids Surf., A* **2002**, *207*, 81–88.
(20) Wolfrum, K.; Lobau, J.; Laubereau, A. *Appl. Phys. A: Mater. Sci. Process.* **1994**, *59*, 605–610.
(21) Xiao, Y.; Yao, Z.; Jin, D.; Yan, F.; Xue, Q. *J. Phys. Chem.* **1993**, *97*, 7072–7074.
(22) Elzein, T.; Bistac, S.; Brogly, M.; Schultz, J. *Macromol. Symp.* **2004**, *205*, 181–190.
(23) Kumaran, N.; Donley, C. L.; Mendes, S. B; Armstrong, N. R. *J. Phys. Chem. C* **2008**, *112*, 4971–4977.
(24) Pan, Y. L.; Wu, Y. J.; Chen, L. B.; Zhao, Y. Y.; Shen, Y. H.; Li, F. M.; Shen, S. Y.; Huang, D. H. *Appl. Phys. A: Mater. Sci. Process.* **1998**, *66*, 569–573.
(25) Ryczkowski, J. *Catal. Today* **2001**, *68*, 263–281.
(26) Evans, J. C. *Inorg. Chem.* **1963**, *2*, 372–375.
(27) Lesieur, P.; Vandevyver, M.; Ruaudel-Teixier, A.; Barraud, A. *Thin Solid Films* **1988**, *159*, 315. Möbius, D.; Orrit, M.; Grüniger, H.; Meyer, H. *Thin Solid Films* **1985**, *132*, 41.
(28) Smith, W.E.; Rospendowski, B.N. Raman Spectra of Phthalocyanines. In *Phthalocyanines: Properties and Applications*, Leznoff, C.C., Lever, A.B.P., Eds.; VCH Publishers: Weinheim, Germany, 1993; Vol. 3, pp 167−225.
(29) Jennings, C. A.; Aroca, R.; Kovacs, G. J.; Hsaio, C. *J. Raman Spectrosc.* **1996**, *27*, 867–872.
(30) Aroca, R.; Jennings, C. A.; Loutfy, R. O.; Hor, A. *J. Phys. Chem.* **1986**, *90*, 5255–5257.
(31) Pasimeni, L; Meneghetti, M; Rella, R; Valli, L; Granito, C; Troisi, L. *Thin Solid Films* **1195**, *265*, 58–65.
(32) Manno, D.; Rella, R; Troisi, L.; Valli, L. *Thin Solid Films* **1996**, *280*, 249–255.
(33) Pasimeni, L; Segre, U.; Toffoletti, A.; Valli, L.; Marigo, A. *Thin Solid Films* **1996**, *285*, 656–658.
(34) Evenson, S. A.; Badyal, J. P. S.; Pearson, C.; Petty, M. C. *Adv. Mater.* **1997**, *9*, 58–61.
(35) Schwartz, D. K.; Garnaes, J.; Viswanathen, R.; Chiruvolu, S.; Zasadzinski, J. A. *Phys. Rev. E* **1993**, *47*, 452–460.